A Novel Improved Stable Power Supply Model Intended to Industrial Appliances Based on the Magnetic Flux Leakage Transformer

H. Outzguinrimt, M. Lahame, M. Chrayagne[1], R. Oumghar, B. Bahani[2]

Abstract – **The current paper investigated an improved three-phase Magnetic Flux Leakage Transformer (MFLT) comprising a magnetic circuit of the core-type, intended for supplying electrical energy to the power circuits of microwave ovens. It is widely used to stabilize the electric current in the supply of electrotechnical equipment, in particular for the case of the high voltage power supply. In this paper, a novel contribution to a new iron core structure instead of shell-type, which often exists in electrotechnical devices, is presented. Thereafter, this new model provides a stabilized state after a drastic change in the load or the voltage of the supply network. An approach is used to model the electric circuit of the Core-Type Transformer (CTT). The duality of the electric circuit and the magnetic circuit can generate a model that considers the design and construction characteristics of the transformer. Thus, detailed circuit analysis using a reluctance network method is given, thereby its performance is evaluated for an 800W/2450MHZ magnetron. At last, a newly developed method describes an approach for modelling the nonlinear inductances by an analytic expression under the MATLAB-SIMULINK® code. It deduced by an analytic fitting of the nonlinear B-H curve. As a result, the waveforms simulations are consistent with the experiments in the case of the conventional power supply used in a microwave oven. Detailed design and implementation procedures are presented in the following sections, including the design of the new power supply.**

Keywords – **Microwave ovens, Modelling, Core-type transformer, Magnetron, Power supply.**

I. INTRODUCTION

The development of the industrial heating system has very quickly outstripped the domestic microwave ovens in recent years [1]. Nowadays, more and more, the microwave processes are implanted in the industrial field. Numerous studies focus again on this axis [2]-[3], especially for the high temperature like heat treatment of materials. Also, recent research focuses on new industrial microwave systems that have already progressed in specific industrial sectors, such as the food industry [4]-[5], which uses them to defrost, pasteurize, or pre-cook. It can use it also in certain applications, like drying and extracting solvents. Furthermore, microwaves have a benefit to be improved and more developed; this technology is promoted with a bright future.

This research is a part of the development contribution relating to the manufacturing industry of high voltage stable power supplies. More specifically, it is interested in studying a new three-phase high voltage power supply intended for industrial, scientific, and medical appliances. Usually, the conventional power supplies are based on MFLT in concert with a high voltage capacitor, a high voltage diode. This combination caused a constant current to be delivered to the magnetron over the normal range of line voltages [6]-[7]. The MFLT are the essential components of those power supplies and electrical circuits. They are manufactured and used for a long time; hence they must be well studied and understood. The studies done on this type of transformer had significantly contributed to the remarkable progress made in the field of stable power supplies, particularly the supply of magnetron for industrial microwave generators [8-13]. Nevertheless, a few written references on the physical details of their operation, and little documentation on their characterization can be found in the available literature. Due to those factors, we continuously innovate to offer and develop a new model of three-phase high voltage power supplies.

In the past years, many studies deal with the design of Shell-Type Transformers (STT), which are commonly employed in power supplies. Chraygane et al. [14] studied the first classical design of a high voltage power supply for the magnetron model using a single-phase MFLT with a shell-type core. This work is done by adopting the π-equivalent of shunts transformer, taking the saturation phenomena, and the stabilization process of the magnetron current into account. Accordingly, this mode seems more convenient to use by software tools, and it was tested by E.M.T.P software (Electro-Magnetic Transients Program), near the nominal state. Ouled Ahmedou et al. [15] suggested a new approach for modeling the nonlinear inductances by an analytic expression under the MATLAB environment. The current representation of these nonlinear inductances is based on Lookup Table technique (LUT). So far, Bassoui et al. [16] and Lahame et al. [17] developed a new original fuzzy model using the Adaptive Neuro-Fuzzy Inference System (ANFIS).

The model proposed a new diagram block of nonlinear inductance to model the magnetization curve B(H) of the ferromagnetic material of the transformer. At last, Oumghar et al. [18] conducted a more detailed study on possible and achievable geometric configurations of a single-phase

Article history: Received August 23, 2021; Accepted December 27, 2021

H. Outzguinrimt, M. Lahame and R. Oumghar are with the National School of Applied Sciences, ENSA, Ibn Zohr University, Morocco, E-mails: hamid.outzguinrimt@edu.uiz.ac.com, M.lahame@edu.uiz.ac.ma, raja.oumghar@edu.uiz.ac.ma

[1]M. Chrayagne is with the Agadir High School of Technology, MSTI Research Team, Ibn Zohr University, Agadir, Morocco, E-mail: m.chrayagne@uiz.ac.ma

[2]B. Boubker is with laboratory of engineering sciences and energy management (LASIME), in the national school of applied sciences (ENSA), Agadir, Morocco, E-mail: b.bahani@gmail.com

transformer with a single magnetic shunt. The dimensioning of the construction parameters of the MFLT were detailed for each geometrical configuration by checking the constraints and ensuring the conditions imposed by the manufacturer of the magnetron. This proposed study showed that this model dimensioned correctly to provide the same nominal operation of the magnetron, thus delivering its full nominal microwave power.

Broadly classifying, the core construction can be separated into core-type and shell-type. Although various studies on stable power supplies operation modeling from different aspects and different techniques have been reported [19-22], almost all of them have included the STT form into the modeling and simulation. At present, the innovation proposed in this work is a new model of the CTT with specific geometric parameters, while ensuring the proper functioning of the magnetrons. The idea is to use the previous models in the case of a single-phase [23],[24], and exploit them to be suitable for a new model in the three-phase. Generally, the new model must be able to operate and oscillate under the same conditions as the magnetrons (800 W, 2.45 GHz) as that of conventional power supply generators.

Moreover, the design of the CTT model is equipped with a single shunt instead of two shunts. Obviously, the main advantage of the proposed core design, it presents an easy construction, has low mechanical resistance in the reason for the non-bracing of the windings, as well as the set can be easily removed mounted for repair work, presents a better heat dissipation of the windings and best suited for EHV (Extra High Voltage) requirements. Unlike the STT, which is characterized by high mechanical resistance, cannot be easily disassembled for work repair, the heat does not dissipate windings easily as it is surrounded by core, and it is not suitable for EHV (Extra High Tension) [25]. Detailed descriptions of transformer construction and operation are present in the following sections.

II. DESCRIPTION OF SYSTEM DESIGN

First and foremost, the CTT is a typical structure used for stable power applications. The design is fabricated by superimposes three single-phase transformers in which the cores and windings for all three phases are merged into a single core structure. The core is SF_{19} which has a nonlinear characteristic and its structure is E-I type. In general, the CTT has three separate windings: a line voltage primary winding, a high voltage secondary winding, and a low voltage filament winding, this latter, may be removed, as it would no longer be used in this work. The primary and secondary windings are wound in the outer of the core columns. There are three vertical shunts, only one shunt for each phase composed of silicon steel sheets and located in the center leg. Hence the importance of shunts is to provide a magnetic flux path, which is rolled in the direction to reduce the loss of iron. As well as, the flux leakage in magnetic shunts could not be ignored; it is considered as a constant leakage inductance in equivalent circuit analysis [26]. Between the shunt and the core, there is an air gap that allows different densities of flow to be obtained in the primary and secondary parts of the central leg. The secondary voltage can be stabilized by the characteristic of the main magnetic circuit saturation and non-saturation property of the leakage branch.

A. Power Generator

Fig. 1 shows a basic power block diagram for the power supply. The primary winding of each phase is directly connected to the AC voltage power. The high voltage capacitor, in conjunction with the diode, forms a voltage-doubler rectifier circuit, which boosts the voltage at the magnetron to almost 4000V DC. The design of magnetron consists of the filament supply with low voltage 3.3 V/12A Alternating current (AC) power supply to heat the filament of magnetron by flowing current through it, and a separate high voltage −4kV/0.66A Direct Current (DC) power supply provides bias to the cathode. The secondary winding provides high voltage for the magnetron anode and ensures the stabilization of the average anode current (I_{averg}= *300mA*) due to the saturation of its magnetic circuit. The anode voltage must be large enough to activate the magnetron. Moreover, if the anode voltage fluctuates, the anode current changes distinctly, even making the magnetron stop working. Thus, it is clear that the power supply must have some form of regulation that stabilizes the power output of the magnetron.

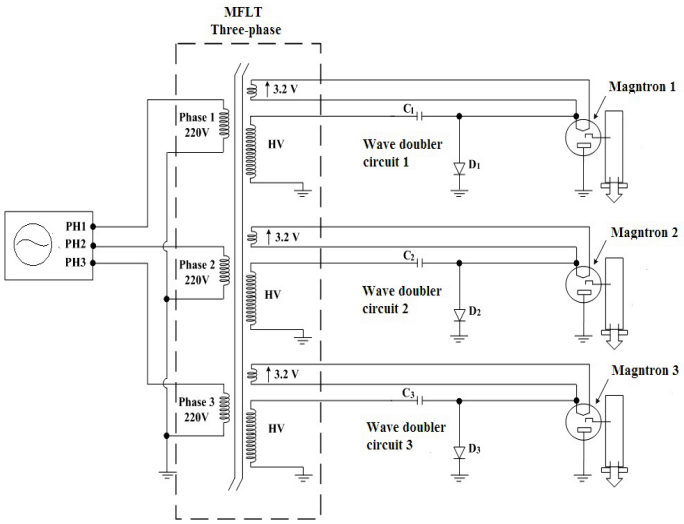

Fig. 1. Scheme of the three-phase HV power supply of a magnetron per phase.

III. CORE DESIGN

A. Construction Details of the Core-Type Transformer

The dimensions of the CTT are shown in Fig. 2. The main geometrical dimensions of the transformer core include an overall width frame (W) and an overall height frame (H), the window height (H_w), the window width (W_w), the outer and central limbs. Windings include the section area and the number of turns. Besides, the sizes of the winding conductors mainly depend on the choice of current density.

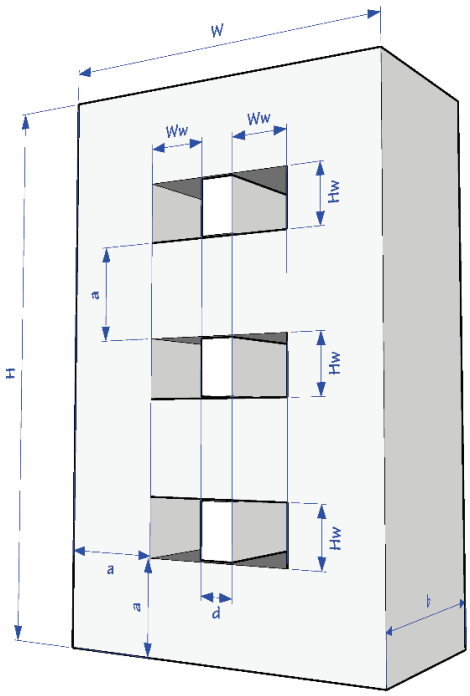

Fig. 2. Main dimension of magnetic frame.

The design constants of this design procedure are selected, taking all the geometric considerations and the imposed constraints [18]. To limit the number of geometric parameters, we admit that the parameter "*a*'" defines the width of the unwound core, "*b*'" represents the depth of core, and "*d*" defines the width of the equivalent shunt stack. According to Fig. 2, the relevant core parameters used in MFLT design are given in Table I.

TABLE I
PARAMETERS USED IN MFLT DESIGN

Symbols	Parameters	Units	Values
a	Width of outer limb	mm	38.5
b	Depth of core	mm	78
H	Overall Height	mm	226
W	Overall Width	mm	138.5
d	Height of shunt	mm	13.9
H_w	Height of window	mm	23.8
W_w	Width of window	mm	24
d_p	Primary Conductor Diameter	mm	1.5
d_s	Secondary Conductor Diameter	mm	0.46
S_p	Primary Winding Cross Section	mm^2	1.75
S_s	Secondary Winding Cross Section	mm^2	0.165
i_{prms}	Primary Current	A	7
i_{srms}	Secondary Current	A	0.66
n_1	Primary Windings	turns	224
n_2	Secondary Windings	turns	2400

B. Main Dimension of Window Area and Core Proportion

Similar to shell-type, the windings cross-sectional area is rectangular. The dimensions of windows define the winding area, number of layers, and the height of the windows. Moreover, the size of windows for the CTT must be sufficient to accommodate all the turns of the primary and secondary windings. So, we compared the widest of the transformer window with the space occupied by the windings primary and secondary (see Fig. 3). Whereas the number of possible windings in each column on the primary side (respectively secondary side) is obtained by calculating the wire diameter corresponding to each side.

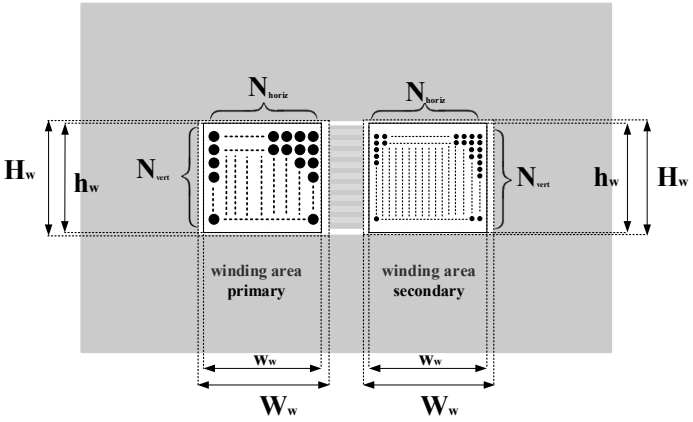

Fig. 3. Illustration of windings primary and secondary arrangement.

C. Winding Layout

One widely method used in determining the windings area, is to define the ratio k_b called "fill factor", which is the total area occupied by the copper material of the windings in the window area. The first step, is calculating the winding coefficient, in practice k_b is between 0.3 and 0.7, it never exceeds these values. The fill factor can be calculated from:

$$k_b = \frac{n \times \pi \times r^2}{S_w} \tag{1}$$

Where n is the number of turns of the coil, and S_w is the cross-section of the window.

For the primary side window, the winding coefficient is:

$$k_b = \frac{224 \times 1.75}{571.68} = 0.685 \prec 0.7 \tag{2}$$

Thus, for the secondary side window, the winding coefficient:

$$k_b = \frac{2400 \times 0.165}{571.68} = 0.692 \prec 0.7 \tag{3}$$

We conclude from the values of the coefficient k_b obtained in Eq. (2) and Eq. (3) that the coil body supports the windings. The next step is to calculate the number's turns of wire, that can fit in each layer of winding for each different winding,

deviating the height of the window (H_w) by the diameter of each wire (Eq. (4) and Eq. (5)):

$$N_{\text{Vert}}^{\text{p}} = E\left(\frac{H_w}{d_p}\right) = E\left(\frac{23.8}{1.5}\right) = 15 \tag{4}$$

$$N_{\text{Vert}}^{\text{s}} = E\left(\frac{H_w}{d_s}\right) = E\left(\frac{23.8}{0.46}\right) = 51 \tag{5}$$

where E (X) is the integer part of X.

Then, from the number of windings per column of each window on the primary side (respectively secondary), we can calculate the number of vertical layers necessary for wind n_1 turn (respectively n_2 turn). It suffices to divide the number of primary turns n_1 (or secondary n_2) by the number of windings per column of each window (Eq. (6) and Eq. (7)):

$$N_{\text{hori}}^{\text{p}} = E\left(\frac{n_1}{N_{\text{Verti}}^{\text{p}}}\right) = E\left(\frac{224}{15}\right) = 14 \tag{6}$$

$$N_{\text{hori}}^{\text{s}} = E\left(\frac{n_2}{N_{\text{vert}}^{\text{s}}}\right) = E\left(\frac{2400}{51}\right) = 47 \tag{7}$$

We define:

$$R_{rest} = n - N_{\text{Vert}} \tag{8}$$

$$R_{rest} = \begin{cases} 0 \Rightarrow n = N_{Vert} \\ \text{otherwise} \quad \Rightarrow N_{vert} = N_{Vert} + 1 \end{cases} \tag{9}$$

For the two cases ($n_1 - N_{\text{Vert}}^{p} \neq 0$, $n_2 - N_{\text{Vert}}^{s} \neq 0$), this allows us to choose the second case of Eq. (9). The values are given:

$$N_{vert}^{p} = N_{\text{Vert}}^{\text{p}} + 1 = 15 \tag{10}$$

$$N_{vert}^{s} = N_{\text{Vert}}^{\text{s}} + 1 = 48 \tag{11}$$

Finally, to verify the design confirm of this transformer, it must reassure that the height winding h_{pw} and h_{sw} are fit in the allowable window height of H_w to check that the primary and secondary winding can enter the carcass of each phase, this makes it possible to manage the winding space, thus exploiting the geometry of the windings:

$$h_w \leq \pi \times r \times N_{vert} \tag{12}$$

If this condition is not satisfied, it is necessary to return to the first step, to Eq. (1), in order to recalculate the area product changing the value of the parameter k_b. In what follows we check this constraint to validate these parameters, based on Eq. (12), we calculate the height winding primary (h_{pw}) and secondary (h_{sw}).

$$h_w = \begin{cases} h_{wp} = N_{vert}^{p} \times d_p = 22.5mm \prec 25mm \\ h_{ws} = N_{vert}^{s} \times d_s = 22.08mm \prec 25mm \end{cases} \tag{13}$$

We can conclude from Eq. (13) that the geometry of the equivalent transformer may realizable. Fig. 4, indicates the main dimensions (in mm) of the window for the primary and secondary windings.

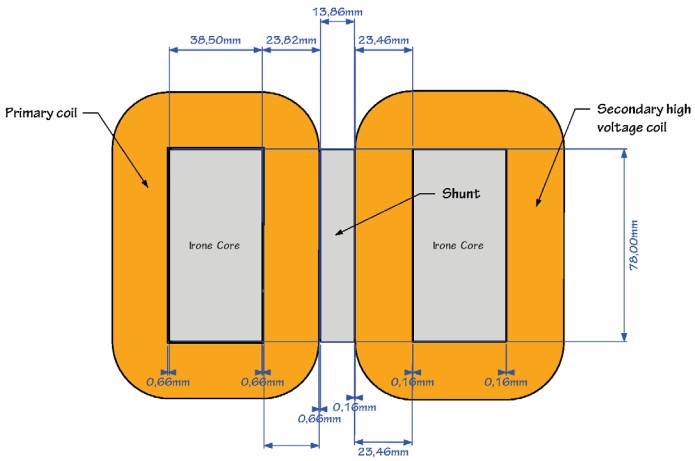

Fig. 4. The geometrical arrangement of primary and secondary windings in a transformer window.

IV. Core Design

In this part, the method establishes a transformer core model using the duality principle between magnetic and electrical circuits is presented. Thus, the method allows to study and analysis of a magnetic circuit without having to write the coupled equations of the magnetic circuit. Tick with an analogy of an electrical circuit. So, an electrical circuit can be built from a magnetic circuit based on the topological method of Colin Cherry [27].

A. Equivalent Magnetic Circuit

In the literature, the analytical magnetic modeling of a transformer accomplishes most of the time by an equivalent magnetic circuit, also named simply reluctance circuit approach. To find the analytical model, firstly we suppose that all the magnetic fluxes are enclosed to the magnetic material of the core, and the leakage fluxes in the air paths around the windings are negligible. Thus, to discretize the geometry of the transformer into a network of reluctances, the magnetic core of the transformer is divided into different sections respecting uniform fluxes of each transformer phase. Each section is represented by its reluctance, which provides a relation between the corresponding flux ϕ and the magneto-motive forces F. Therefore, this method allows us to build a network of reluctances from the core structure and characteristics of the magnetic equivalent circuit as shown in Fig. 5.

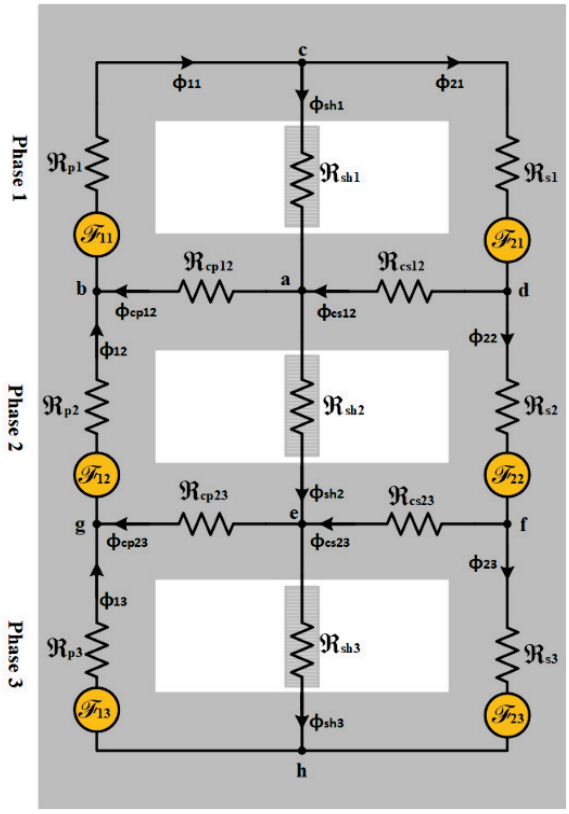

Fig. 5. Magnetic equivalent circuit of a CTT structure with path of the main magnetic flux.

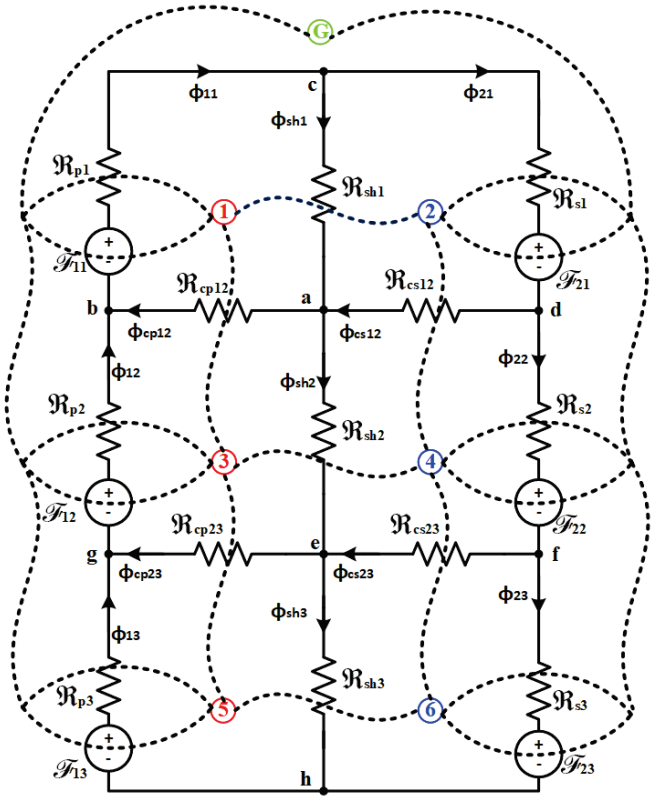

Fig. 6. Topological development of equivalent magnetic circuit of a transformer core

$\phi = \{\phi_{1j}, \phi_{2j}, \phi_{3j}\}$ is a magnetic flux confined to the iron core, $\phi_c = \{\phi_{cp12}, \phi_{cs12}, \phi_{cp23}, \phi_{cs23}\}$ are magnetic fluxes flowing in the common core between phase 1-2 and phase 2-3, and ϕ_{shj} is magnetic flux flowing in a stack of shunts. $\Im = \{\Im_{1j}, \Im_{2j}\}$ are resultant magneto-motive forces on the transformer legs for j-phase. In the entire text, j denotes the number of the phase studied, where j ∈ [1, 2, 3].

B. Equivalent Electrical Circuit Referred to the Secondary

According to the topological principle of duality, the equivalent electrical circuit of the CTT is derived directly from its magnetic circuit. Consider the equivalent magnetic circuit of the core in Fig. 6. The circuit contains six internal meshes. In each mesh of the magnetic circuit, we define a set of points. An additional reference point (G) is marked outside the circuit.

These points are the nodes of the dual network. Continuous lines join each pair of points; each line crosses through a reluctance. Indeed, an inductance is inserted between the corresponding nodes of the equivalent electrical circuit. The magnetic meshes (abca), (abgea) and (eghe) on the primary side, become the electrical nodes (1, 3 and 5) respectively; thus, the magnetic meshes (acda), (adfea) and (efhe) on the secondary side become the electrical nodes (2, 4 and 6) respectively. The outer magnetic mesh (hgbcdfh) is dual to the node of mass (G). Finally, the graphically derived global equivalent electrical circuit of the core is shown in Fig. 7, where the corresponding nodes are marked.

V. Implementation of a Nonlinear Inductance

A. Fitting Curve B-H by Method Polynomial Function

In this part, we present a simple mathematical expression, which enables the representation of the magnetization curve for the material used SF_{19}. The magnetization curve normally has 3 parts – initial linear zone, knee zone, and saturated zone. The problem has been to cover all operation data from the origin to saturation by a single function, with a minimum error over the whole range to obtain more accurate curve fitting. Serval formulas have been proposed [28], such as approximations by power series, transcendental functions, Fourier series, and by hyperbolas in the form of Froehlich's equation, to represent the B (H) curve, and to judge the quality of the approximation.

Curve fitting is a technique of analyzing an experimental curve, consisting in constructing a curve from a mathematical function and adjusting the parameters of this function to approximate the measured experimental curve [29], provided by the manufacturer of magnetic sheets of ferromagnetic

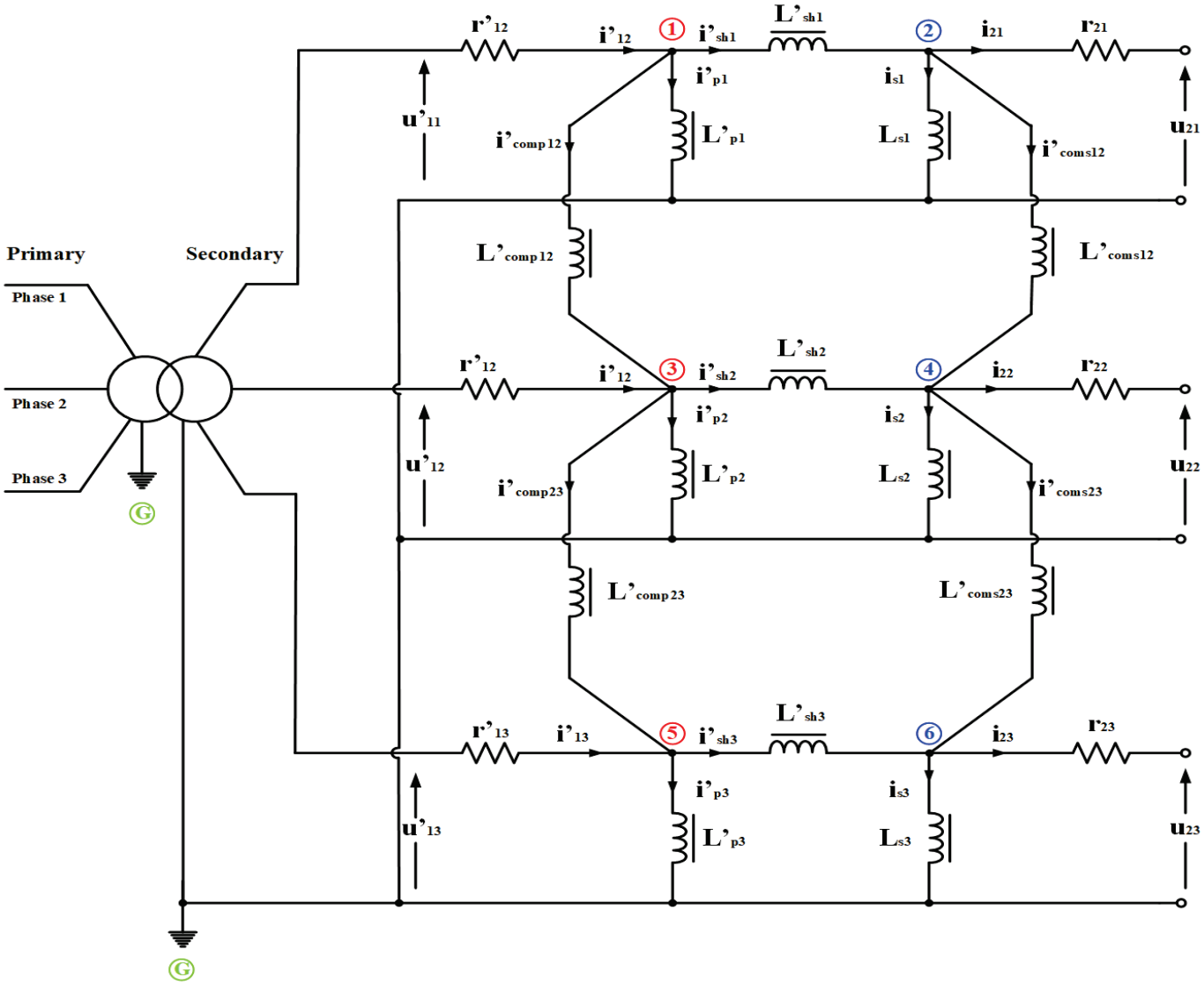

Fig. 7. Equivalent model of the MFLT referred to the secondary.

materials SF_{19} used in the manufacture of the transformer. Each zone (Linear, Knee, and Saturation) is fitted by a polynomial function based on the method of least square.

$$H(B) = \sum_{p=0}^{2} a_{2p+1} B^{2p+1} \tag{14}$$

The constants "a" can be determined by curving fitting methods, using the "polyfit" function in MATLAB boxes. The resulting expression of H is given, getting the best fit by choosing p=2.

As a result, we reconstructed via vector fitting the curve plotted in Fig. 8. The blue line of the curve plotted represents the considered transformer core smoothed characteristic B(H), and the circles plotted the results of the three analytical equations corresponding to the three zones of curving fitting B (H) used.

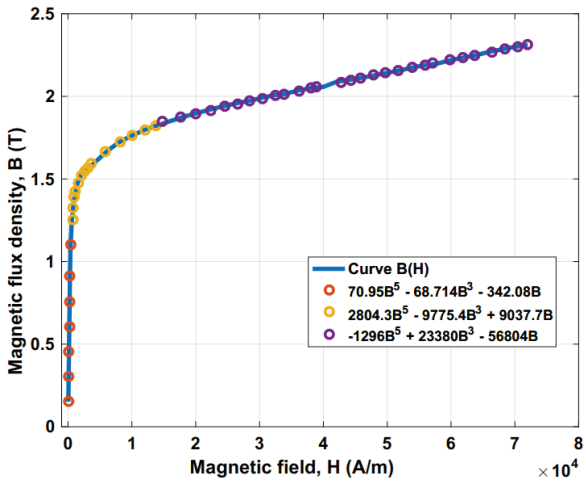

Fig. 8. (–) B–H curve obtained from curve fitting represented by polynomial in comparison with- (o-o) B-H.

B. Nonlinear Inductance Model

During the calculation, it is necessary to represent each nonlinear inductance by its characteristic giving the total flux ($n_2 \cdot \phi(i)$), according to the current $i(t)$. The model of the nonlinear inductance can, therefore, be implemented as a controlled current source, where current (i) is a nonlinear function of voltage (v). Therefore, two Simulink blocks are used. One of them is applied as an integrator block, used to compute the flux from the voltage input. The other one is a function block that implements the saturation characteristics $i = f(\phi)$. All the elements used to build the nonlinear model have been grouped in a subsystem named nonlinear inductance as shown in Fig. 9.

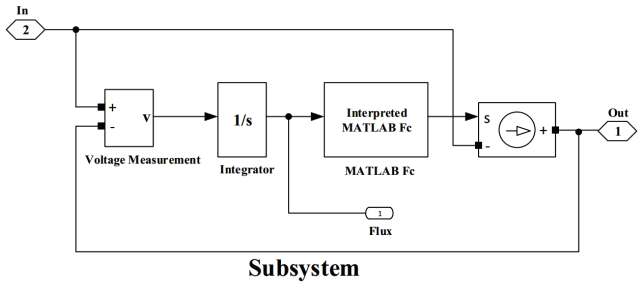

Fig. 9. The equivalent subsystem of a nonlinear inductance.

VI. Validation of the Equivalent Electrical Model

A. Simulink Model

The Simulink model of the π-equivalent circuit diagram is illustrated in Fig. 10. The proposed transformer is rated as 1650VA. The input voltage source is 50Hz, 220 V sinusoidal AC voltage with a ±10% regulating range. The secondary voltage is 2230V. The transformer has three phases, two limbs, the silicon steel used for the iron core material is SF_{19}. A voltage-doubler capacitor C=0.9μF and high voltage rectifier diode D_1. The magnetron is represented by its equivalent diagram deduced from its characteristic electric. It consists of a series-connected ideal diode with a threshold voltage E of approximately 3800 volts and a resistor whose value corresponds to the dynamic resistance 350 ohms of the magnetron [30], [31]. The designed transformer has been simulated in MATLAB 2014a.

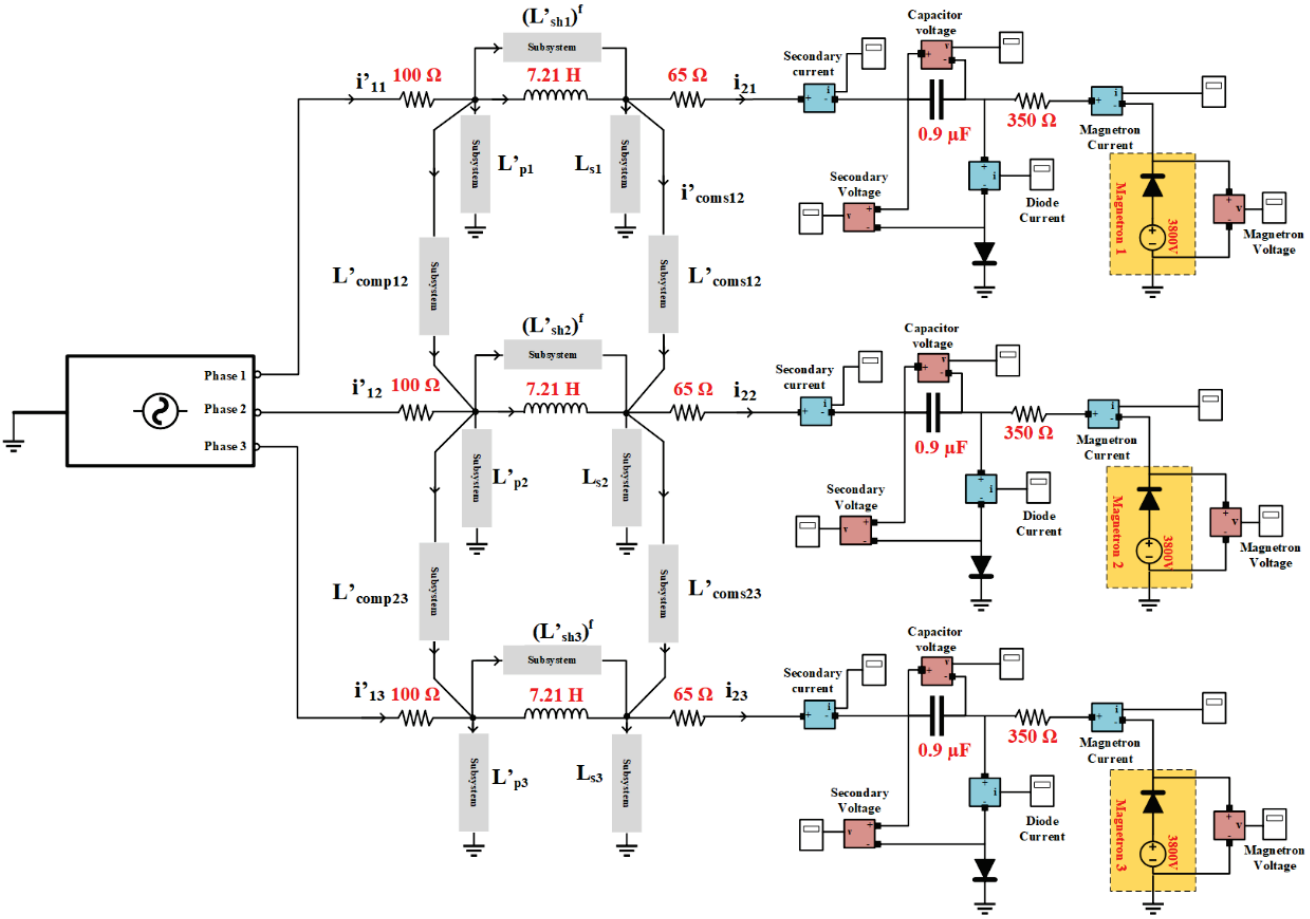

Fig. 10. π-equivalent circuit diagram of the power supply studied for the three-phase transformer designated by n_2 turns

B. Computational Results and Discussion

Fig. 11 shows transient waveforms of the voltage and the current flowing through the magnetron for each phase which are not continuous and exhibits a very large ripple. The waveforms are simultaneously plotted, an offset of $2\pi/3$ is recorded between i_{m1} and i_{m2}, and an offset of $4\pi/3$ is noted between i_{m1} and i_{m3}. Thus, the current cross the magnetron grows up to a maximum of (-1A), decreases and cancels, then increases again. As well as for magnetron voltage increases to a maximum of (-4000A), drops and cancels, then rises again. As a matter of fact, we note that when the current or the voltage is canceled in a phase, it does not cancel in the two other phases; therefore, continuity of service is assured.

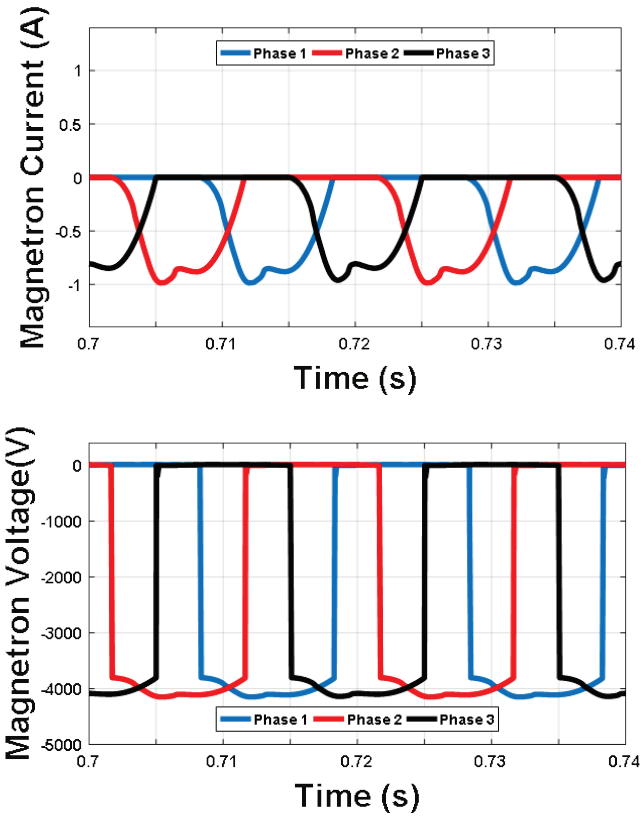

Fig. 11. Simulation results of currents and voltages forms obtained at the magnetron terminal

Fig. 12 shows transient waveforms of the current on the diode, and the voltage on the capacity terminal in each phase. The currents for the three phases are simultaneously traced. It is observed that each diode current D_1 increases up to a maximum of 1A, decreases, and cancels, then increases again. The voltage on the capacity terminal varying between -V(-1500V) and +V(+5500V). The +5500V level is obtained during the conduction of the diodes, while the -1500 V level is obtained during the opposite direction of the current of the diodes D_1. Furthermore, when the voltage and the current are canceled in a phase, the other two phases function normally.

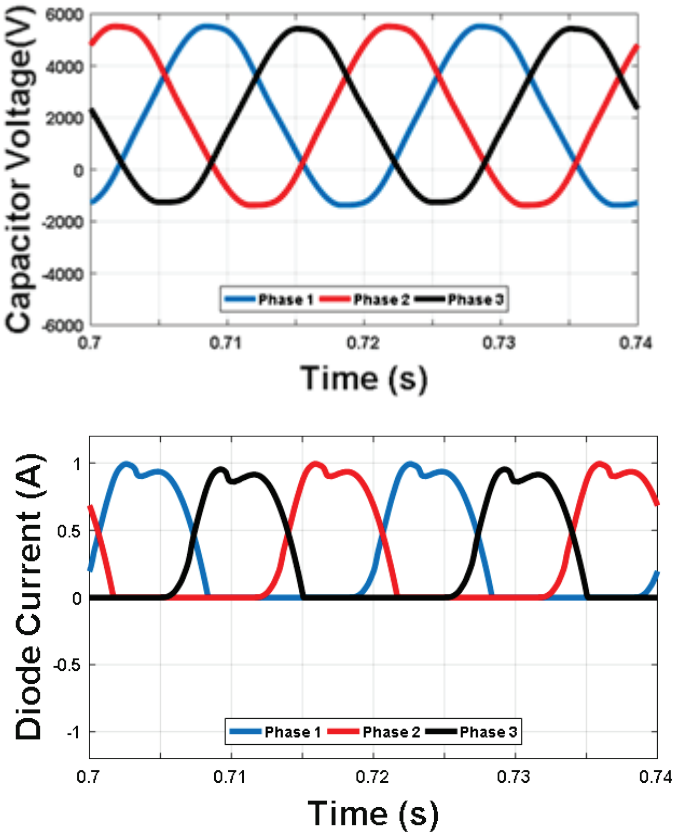

Fig. 12. Simulation results of currents at the capacitor and voltages at the diode forms.

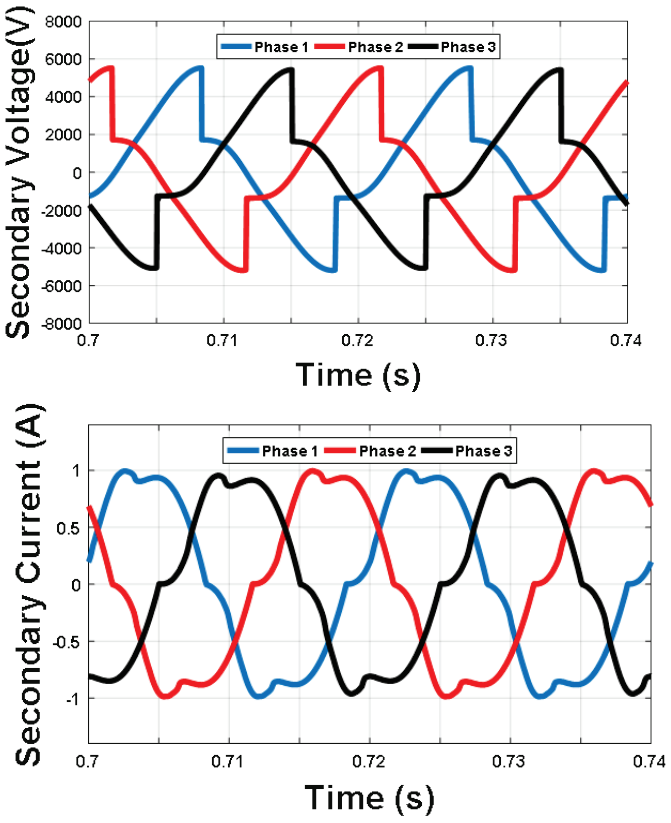

Fig. 13. Simulation results of currents and voltages forms obtained at the secondary terminal.

Fig. 13 illustrates transient waveforms of the secondary current varies between -I(-1A) and +I(+1A), and the secondary voltage varying between -V(-5500V) and +V(+ 5500V). The currents for the three phases are simultaneously traced, a shift of 2π/3 is recorded between i_{s1} and i_{s2}. The same a shift of 4π/3 is noted between i_{s1} and i_{s3}, thus the voltage of phase 2 is offset from that of phase 1 by an angle 2π/3, and as for that of phase 3, it is offset by 4π/3.

As a result, on comparison of these waveforms, it is evident that the use of the proposed CTT model improves the results, and a very good agreement with the recorded experimental voltage and current of the conventional power supply is achieved [32]-[33]. Accordingly, the above results show that the proposed approach is extremely good for modeling power transformers with the analytical method proposed.

C. Verification of the Current Regulation Process in the Magnetrons

During the simulation of this three-phase HV power supply, we managed to observe the stability of the current variations in each magnetron towards the mains voltage. Fig. 14 shows the identical waveform of the current in each magnetron for the respective cases of 200V and 240V (± 10% of the supply voltage 220V).

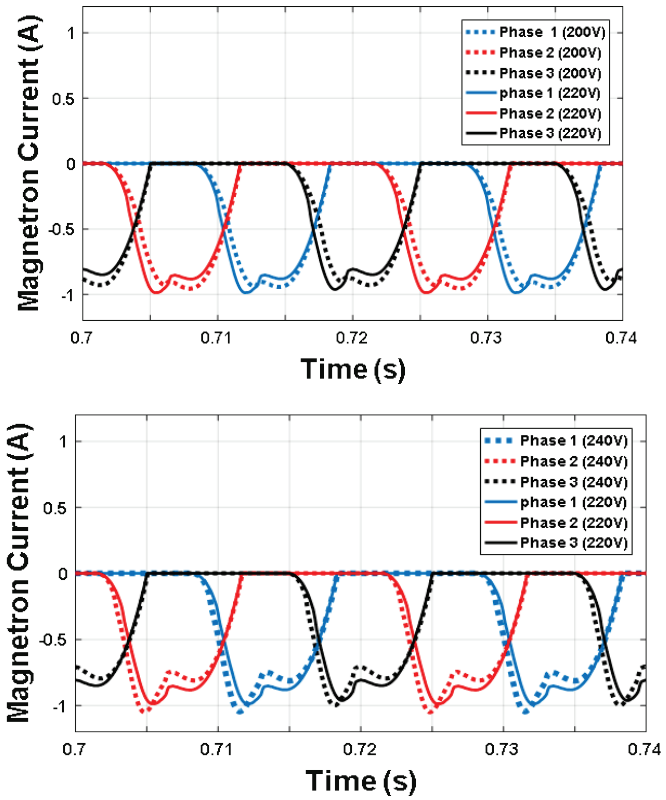

Fig. 14. Stabilization of the anode current in each magnetron concerning variations in the mains voltage by ± 10% of the nominal voltage.

From the results of the simulations obtained, it appears that the current passing through the magnetron in each phase is quite sensitive to any variation of the mains voltage sources. Hence, it is concluded that the current in both cases does not exceed the admissible value for the manufacturer (<1.2 A). So, the model is valid and can operate in good conditions.

VII. CONCLUSION

In this paper, we have made the description and detailed discussion of the modeling and simulation of CTT. This new technology allows discovering another generation of three-phase transformers with a single shunt, which serves to replace the STT. Semi-analytical simulations make this proposition useful, and we can use it in other studies. As a perspective, we aim to get an optimal high voltage magnetic flux leakage transformer design of a three-phase CTT to minimize the total mass and reduce the volume of the transformer. Then study the thermal behaviour of a three-phase MFLT under load conditions with the finite element analysis.

REFERENCES

[1] R. A. Shute, "Industrial Microwave Systems for the Rubber Industry", *Journal of Microwave Power*, vol. 6, no. 3, pp.193-205, 1971.

[2] S. R. Jang, H. J. Ryoo, S. H. Ahn, J. S. Kim and G. H. Rim, "Development and optimization of high-voltage power supply system for industrial magnetron", *IEEE Transactions on Industrial Electronics*, vol. 59, no.3, pp. 1453-1461, 2012.

[3] A. I. Zemtsov and I. I. Artyukhov, "Power Supply System for Industrial Packaged Magnetrons Group", *29th International Conference Radioelektronika (RADIOELEKTRONIKA)*, pp. 1-5, 2019.

[4] S. Limhengha, S. Limnararat, I. Jangchud and W. Sriseubsai, "Novel Foodstuff Conveyor Belts Compound for Energy Saving: The Effect of Microwave Pre-Heating and Mixed Fillerson Mechanical Properties", *ARPN Journal of Engineering and Applied Sciences*, vol. 12, no. 4, pp. 1105-1110, 2017.

[5] A. C. Grimm, "RCA 915-MHz Power Oscillator for Microwave Cooking and Industrial Heating Applications", *Journal of Microwave Power*, vol. 4, no.1, pp. 5-10, 1969.

[6] J. E. Gerling, "Microwave Oven Power: A Technical Review", *Journal of Microwave Power and Electromagnetic Energy*, vol. 22, no. 4, pp. 199-207, 1987.

[7] T. Oguro, "Trends in Magnetrons for Consumer Microwave Ovens", *Journal of Microwave Power*, vol. 13, no. 1, pp. 27-35, 1978.

[8] Bahani, M. Chraygane, M. Ferfra, R. Batit, N. El ghazal, A. Belhaiba and M. Bassoui, "Modeling of a new Three Phase High Voltage Power Supply for Industrial Microwave Generators with Magnetron", *International Review on Modelling and Simulations*, vol. 8, no. 3, pp. 362-371, 2015.

[9] M. Chraygane, N. El Ghazal, M. Fadel, B. Bahani, A. Belhaiba, M. Ferfra and M. Bassoui, "Improved Modeling of new Three-Phase High Voltage Transformer with Magnetic Shunts", *Archives of Electrical Engineering*, vol. 64, no. 1, pp. 157-172, 2015.

[10] L. M.R. Oliveira and A. J.M. Cardoso, "Modelling and Simulation of Three-Phase Power Transformers", *Proceedings of the 6th International Conference on Modelling and Simulation of Electrical Machines, Converters and Systems (ELECTRIMACS 99)*, pp. 257-262, 1999.

[11] H. Outzguinrimt, M. Chraygane, M. Lahame, R. Oumghar, R. Batit and M. Ferfra, "Modeling of Three-Limb Three-Phase Transformer Relates to Shunt Core Using in Industrial Microwave Generators with N=2 Magnetron Per Phase", *International Journal of Electrical and Computer Engineering*, vol. 9, no. 6, pp. 4556-5565, 2019.

[12] R. Batit, M. Chraygane, M. Ferfra and B. Bahani, "Failures' Study of a New Character Three-Phase High Voltage Supply for industrial Microwave Generators with one Magnetron per Phase", *Journal of Engineering Science and Technology Review*, vol. 9, no. 1, pp.145-150, 2016.

[13] L. M. R. Oliveira and A. J. M. Cardoso, "Three-Phase, Three-Limb, Steady-State Transformer Model: The Case of a YnZn Connection", *Proceedings of the IASTED International Conference (Power and Energy Systems)*, pp. 467- 472, 2000.

[14] M. Chraygane, "Modélisation et optimisation du transformateur à shunts d'une alimentation haute tension à magnétron pour générateurs micro-ondes 800W-2450Mhz destinés aux applications industrielles", *PhD thesis*, 1993.

[15] M. Ould Ahmedou, M. Ferfra, M. Chraygane, and M. Maaroufi, "A New Modeling of the Nonlinear Inductances in MATLAB", *MATLAB Tool Books*, Chapter 13, 2012.

[16] M. Bassoui, M. Ferfra and M. Chraygane, "ANFIS Modeling of Nonlinear Inductance", *International Conference on Electrical and Information* Technologies (ICEIT), pp. 458-462, 2016.

[17] M. Lahame, M. Chraygane, H. Outzguinrimt, R. Batit, R. Oumghar and M. Ferfra, "Modeling Under Matlab by Anfis of the Three-Phase Tetrahedral Transformer Using in Microwave Generator for Three Magnetrons per Phase", *TELKOMNIKA Telecommunication, Computing, Electronics and Control*, vol. 16, no. 5, pp. 2406-2414, 2018.

[18] R. Oumghar, M. Chrayagne, H. Outzguinrimt, M. Lahame and A. Bouzit, "Contribution to Development of a new Transformer with a Single Magnetic Shunt for Industrial Microwave Generators", *International Journal of Advanced Trends in Computer Science and Engineering*, vol. 8, no. 6, pp. 3438-3446, 2019.

[19] M. Ferfra, M. Bassoui and M. Chraygane, "Transformateur triphasé HT à shunt magnétiques de type tétraédrique pour four à micro-ondes", *Morocco Patent MA 39667 A1*, 2018.

[20] A. Belhaiba, A. Bouzit, N. Elghazal, M. Ferfra, M. Bousseta, M. Chraygane and B. Bahani, "Comparative Studies of Electrical Functioning of Magnetron Power Supply for One Magnetron", *Journal of Engineering Science and Technology Review*, vol. 6, no. 3, pp. 35-40, 2013.

[21] B. Kawkabani and J.-J. Simond, "Improved Modeling of Three-Phase Transformer Analysis Based on Magnetic Equivalent Circuit Diagrams and Taking into Account Nonlinear BH Curve", *Journal Electromotion*, vol. 13, no. 1, pp. 5-10, 2006.

[22] M. Ould Ahmedou, M. Bassoui. M. Ferfra, M. Chraygane, A. Belhaiba, N. El ghazal and B. Bahani, "Global Modeling of a new Three Phase HV Power Supply for Microwaves Generators with N Magnetrons by Phase (Treated Case N=1) Under Matlab Simulink Code", *Journal of Theoretical and Applied Information Technology*, vol. 61, no. 1, pp. 229-238, 2014.

[23] M. Chraygane, M. Teissier, A. Jammal and J.-P. Masson, "Modélisation d'un transformateur à shunts magnétiques utilisé dans l'alimentation H.T. d'un générateur micro-ondes à magnétron", *Journal de Physique III France 4*, vol. 4, no. 11, pp. 2329-2338, 1994.

[24] M. Chraygane, M. Ferfra and B. Hlimi, "Modélisation d'une alimentation haute tension pour générateurs micro-ondes industriels à magnétron", *La Revue 3EI, 41*, pp. 37-47, 2005.

[25] R. Doebbelin, M. Benecke and A. Aindemann, "Calculation of Leakage Inductance of Core-Type Transformers for Power Electronic Circuits", *13th International Power Electronics and Motion Control Conference*, 2008.

[26] H. Outzguinrimt, M. Chraygane, M. Lahame, R. Oumghar, A. Bouzit and M. Ferfra, "Optimal Design of a Three-Phase Magnetic Flux Leakage Transformer for Industrial Microwave Generators", *Bulletin of Electrical Engineering and Informatics*, vol. 9, no. 1, pp. 57-66, 2020.

[27] E. C. Cherry, "The Duality Between Interlinked Electric and Magnetic Circuits and the Formation df Transformer Equivalent Circuit", *Proceedings of the Physical Society. Section B*, vol. 62, no. 2, pp. 101, 1949.

[28] B. Kawkabani and J.-J Simond, "Improved Modeling of Three-Phase Transformer Analysis Based on Nonlinear BH Curve and Taking Into Account Zero-Sequence Flux", *Recent Developments of Electrical Drives*, Springer, Dordrecht, pp. 451-460, 2006.

[29] V. Sandeep, S. S. Murthy and B. Singh, "A Comparative Study on Approaches to Curve Fitting of Magnetization Characteristics for Induction Generators", *IEEE International Conference on Power Electronics, Drives and Energy Systems (PEDES),* pp. 1-6, 2012.

[30] A. I. Zemtsov, I. I. Artyukhov, S. F. Stepanov, E. E. Mirgorodskaya, N. P. Mityashin and N. A. Kalistratov, "Modeling and Simulation of a low Power Magnetron as an Element of Electrical System", *28th International Conference Radioelektronika 2018*, pp. 1-5, 2018.

[31] A. Borisenko, I. Artyukhov, and A. Zemtsov, "Autonomous Power Supply System of Magnetron Generators Group", *2018 2nd School on Dynamics of Complex Networks and their Application in Intellectual Robotics*, pp. 72-74, 2018.

[32] H. Outzguinrimt, A. Bouzit, M. Chraygane, M. Lahame, R. Oumghar and M. Ferfra, "Design and Modeling of a new Configuration of three-phase transformer for high voltage operation using in microwave industrial", *2018 International Conference on Electronics, Control, Optimization and Computer Science (ICECOCS),* pp. 1-6, 2018.

[33] B. Bahani, M. Ferfra, M. Chraygane, M. Bousseta, N. El Ghazal and A. Belhaiba, "Modeling and Optimization of a new Single-Phase High Voltage Power Supply for Industrial Microwave Generators", *International Review of Electrical Engineering*, vol. 9, no. 1, pp. 136-145, 2014.